

Dissolved redox species for the improvement of the performance of supercapacitors

Bamidele Akinwolemiwa^a and George Z. Chen^{a,b,*}

^aDepartment of Chemical and Environmental Engineering, and Centre for Sustainable Energy Technologies, Faculty of Science and Engineering, University of Nottingham Ningbo China, Ningbo 315100, P. R. China.

^bDepartment of Chemical and Environmental Engineering, Faculty of Engineering, University of Nottingham, Nottingham NG7 2RD, UK.

ABSTRACT

The recent surging investigations into the applications of redox active electrolytes for the improvement of charge storage in supercapacitors and other related hybrid devices have shown a lot of promise but also revealed a number of challenges. This review aims at providing a critical analysis of up-to-date research and development in the use of dissolved redox species in electrolytes for supercapacitors. The challenges and confusions inherent in the description of the charge storage metrics, particularly charge capacity and capacitance, are carefully appraised. The role of the carbon electrode properties such as surface area and surface functionality are explained from the standpoint of the interactions of these redox species with the carbon electrode/electrolyte (E/E) interface. Different strategies that have been adopted for the improvement of practical devices using redox electrolytes are reviewed. Furthermore, brief descriptions on some promising progresses in this increasingly important research area are provided.

KEYWORDS: redox electrolytes, supercapacitors, carbon electrodes, nemstian storage, capacitive storage

1. Introduction

Electrochemical energy storage devices have been earmarked as an important component of the drive

to a sustainable energy future, since they find applications in grid storage to support intermittent energy generation from renewable energy sources, electric transport systems, etc. Broadly speaking, batteries and supercapacitors are two very important electrical energy storage devices. Moreover, whilst batteries can be used for high energy storage capacity, that is storing enough energy for a long time, supercapacitors on the other hand can be used to provide high power capability for short duration. In general, practical energy storage systems integrate these devices as discrete components for various applications, for example, in the power systems of hybrid vehicles [1]. Moreover, from a material standpoint, improved energy stores displaying high power and high energy are desirable; in other words the properties of the battery and a supercapacitor can be incorporated into a single cell to achieve optimal performance metrics. One such important device is the supercapattery, which is the integration of a battery and a supercapacitor charge storage mechanism in a single cell [2]. In general, such developments in the field of energy storage have been achieved through the fabrication of composite electrodes, and a classical example is the composite electrode of MnO₂ and carbon nanotubes (CNTs) [2, 3].

Another important component in electrochemical devices is the electrolyte which has received less attention than electrode materials, but can also help in the improvement of charge storage capabilities of electrochemical devices. Particularly

*Email id: george.chen@nottingham.ac.uk

in supercapacitors, the use of electrolytes that are active within the operation voltage of these devices has resulted in significant performance enhancement. Examples of electrolytes that have been used to achieve this additional charge include various quinonoid compounds, e.g. hydroquinone [4], halides, e.g. alkali metal iodides [5], and transition metal ions, e.g. Fe^{2+} and Cu^{2+} [6]. These dissolved redox species (DRS) could be added into supporting electrolytes (i.e. as redox additives) or could themselves be inherently active components of the electrolyte (i.e. redox active electrolytes). They could also be incorporated into polymer electrolytes (i.e. redox polymer electrolytes) [7, 8].

In practice, the use of these dissolved redox species for supercapacitor applications is mainly to improve the charge storage capacities of the device through various redox mechanisms ensuing from the electrolyte, and leading to increased charge density at the “electrode/electrolyte” (E/E) interface. The purpose of this review is to critically appraise the broad range of investigations that have been undertaken in this research area, by giving detailed descriptions of the mechanisms of charge storage and performance evaluation of devices using DRS. Design strategies that have been adopted in practical devices using DRS are described. A brief perspective on the research trend in this fast growing aspect of electrochemical energy storage is also presented.

2. Interfacial reaction mechanisms of dissolved redox species

Consider the reversible redox reaction due to dissolved redox species in the electrolyte:



If this reaction were to occur at the E/E interface of one of the two electrodes in a supercapacitor (SC) such that the electroactive species (O: oxidised specie, R: reduced specie) could be stored in the pores of the electrode, react with surface functional groups or even shuttle electrons between the lattice of redox active electrodes and O or R in electrolyte, then additional charge storage would have resulted. Since O and R could be anions, cations, or electro-sorbed species, the reversibility of the redox reaction e.g. the ease of adsorption/de-sorption on the electrode surface, the ability of the product of the charging reaction to be retained in the pores of the electrode, the pH and temperature of the electrolyte, would all influence the performance of this redox couple for charge storage. Accordingly, the aforementioned factors would thus inform and help the selection of the electrode and redox electrolyte for practical applications.

We now consider figure 1 in which O and R are the oxidised and reduced states of the redox species, respectively. For charge storage to occur, O_{bulk} or R_{bulk} (i.e. reduced or oxidised species in the bulk solution) would initially enter the pores of the

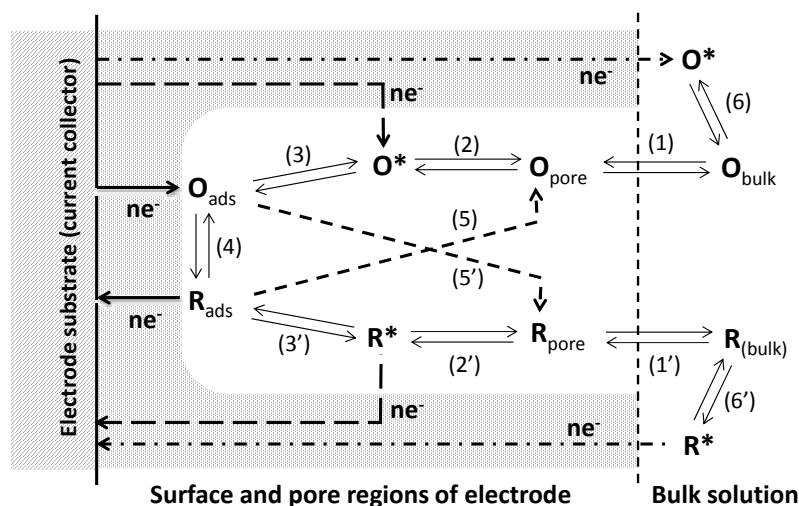


Figure 1. Illustration of possible charge storage mechanisms in the porous carbon electrode of a SC with a redox electrolyte [8] (© The Electrochemical Society, Inc. 2015).

electrode, and this could be accompanied by the equilibria of solvation or de-solvation of the electroactive species during entry to or exit from the pores (Process (1) or (1')). From thermodynamic considerations, it is necessary for redox species in the pore (O_{pore} and R_{pore}) to attain the transition state (O' and R') *via* process (2) or (2') before electron transfer reactions would occur. Furthermore, the electroactive species are then converted from the transition states to the adsorbed states (O_{ads} and R_{ads}) *via* process (3) and (3'), and this process is necessary for interfacial charge storage in SCs. Electron transfer *via* (4) causes the conversion between the adsorbed redox species on the internal and external surfaces of the electrode; this is directly responsible for the enhanced charge storage capacity. It should also be noted that when the redox species are in the transition state, they (O' and R') may also undergo electron transfer reaction without the necessity for adsorption. Further, it is possible that upon electron transfer, the adsorbed species (O_{ads} or R_{ads}) is converted *via* (5) or (5') to a soluble product (O_{pore} or R_{pore}) that can diffuse through the pore and enter the bulk electrolyte. In both cases, if the electron transfer reaction corresponds to the charging process, formation of a soluble product implies that charge storage would be short-lived or not occur because the product of the charging process may diffuse into the bulk electrolyte. Hence, the resulting charge cannot be fully recovered electrochemically - an aggravation of this occurrence is in fact the main cause of high rate of self-discharge for some of these SCs. Conversely, apart from taking place inside the pores, the electron transfer reaction (Process (4)) can also take place on the outer surface of the electrode *via* process (6) or (6'). However, because the outer surface usually possesses a much smaller area than the internal surface of a porous electrode, the contribution from either process (6) or (6') should be insignificant [8].

In general, depending on the surface properties of the electrode material, the redox species could be electro-adsorbed in the electrode material (porous matrix of carbon electrodes) [4, 5, 9] or interact with the reactive edge sites and functional groups on the surface of the carbon material, for example carbonyl groups [6, 10]. Moreover, if the electrode material is pseudocapacitive or battery-like there could be shuttling of the electron transferred in the lattice of the electrode, by the redox species [11].

Also, the dissolved redox species could be such that their charged states form complexes which could be adsorbed on the electrode surface [12].

Furthermore, the redox reaction should be sufficiently reversible in order for the SC with a DRS to display satisfactory charging-discharging properties on repeated cycling (i.e. high cycle stability). One way of ensuring this is to match the concentration of the redox species to that of the supporting electrolyte. For example, the optimal concentration of *p*-phenyldiamine has been shown to be dependent on the concentration of KOH as supporting electrolyte [13]. Important physicochemical properties of the redox species (e.g. ion-solvent interactions) and their effects on the interfacial charge storage properties (e.g. adsorption/desorption) have also been described [14]. Furthermore, since some important redox additives are actually organic-based compounds (e.g. quinones, amides), the effects of substituents on the electrochemical properties of these redox electrolytes have also been investigated [15].

Generally, electrolyte wettability is also important for effective transport of the electroactive species from electrolyte to electrode, and electro-sorption of these redox species [8]. The pore size of the electrodes utilised has also been investigated, and has been used to describe certain interactions of the anionic species with the carbon surface. For instance, the presence of 2-3 nm pores in activated carbon (AC) materials has been claimed as the possible reason for improved charge storage properties of the I_3^-/I^- redox species in acidic media [16]. For instance, the presence of 2-3 nm pores have been used to explain improved charge storage from polyiodides that could be formed from the redox actions of the I_3^-/I^- couple when 10% weight of mesoporous multi-walled carbon nanotubes was mixed with AC electrode [17]. Along these lines, large surface area carbon has also been identified to be important for effective adsorption of such anions [18]. As is expected for all electrochemical devices, there is the need for improved electron and ion transport in the porous electrode materials, and also a reduced charge transfer resistance at the E/E interface [8]. In practice, developing monolithic binder-free carbon coatings on electrodes, engineering the nanostructure of electrode materials to accommodate desirable functional groups, etc. are some means in which electrode surfaces could be optimised to improve the performance of redox-active electrolytes in SCs [19].

3. Electrochemical description of the charge storage mechanism of dissolved redox species

Fundamentally, the application of dissolved redox species in SCs is to obtain more charge at the E/E interface. Consider the total charge at the E/E interface given by the equation:

$$Q_T = Q_{\text{electrode}} + Q_{\text{electrolyte}} \quad (2)$$

where, Q_T is the total interfacial charge, $Q_{\text{electrode}}$ is the charge contribution due to the electrode, and $Q_{\text{electrolyte}}$ is the charge contribution from the dissolved redox species. It should be pointed out that $Q_{\text{electrode}}$ in this case could either be due to electrical double layer (EDL) capacitance or pseudocapacitance, depending on the nature of the electrode used. For example, for EDL capacitance it is generally accepted that this is due to the charge stored at the interface when the carbon electrode is electro-neutralised by the counter-ions from the electrolyte [20]. Furthermore, if the charge storage properties of the electrode can be described with the aid of

the band model for semiconductor which allows continuous addition or removal of electrons from a wide band of energy levels with very small differences, then a pseudocapacitive (i.e. faradaic capacitive) mechanism ensues [2, 3]. It should be noted that from the standpoint of the electrode materials, there are three different charge storage mechanisms, namely; non-faradaic capacitive (EDLC), faradaic capacitive (pseudocapacitance), and non-capacitive faradaic (battery-like or nernstian). Although the EDLC and pseudocapacitive mechanisms are fundamentally different, still their experimental observation gives rise to rectangular cyclic voltammogram (CV) and triangular galvanostatic charge-discharge (GCD) profiles. Moreover on the addition of redox species into the electrolyte the CV or GCD would be very likely battery-like (i.e. non-capacitive faradaic). This is because in general redox additives dissolved in solution would have the redox reaction around a certain potential (the formal redox potential) (see Figure 2).

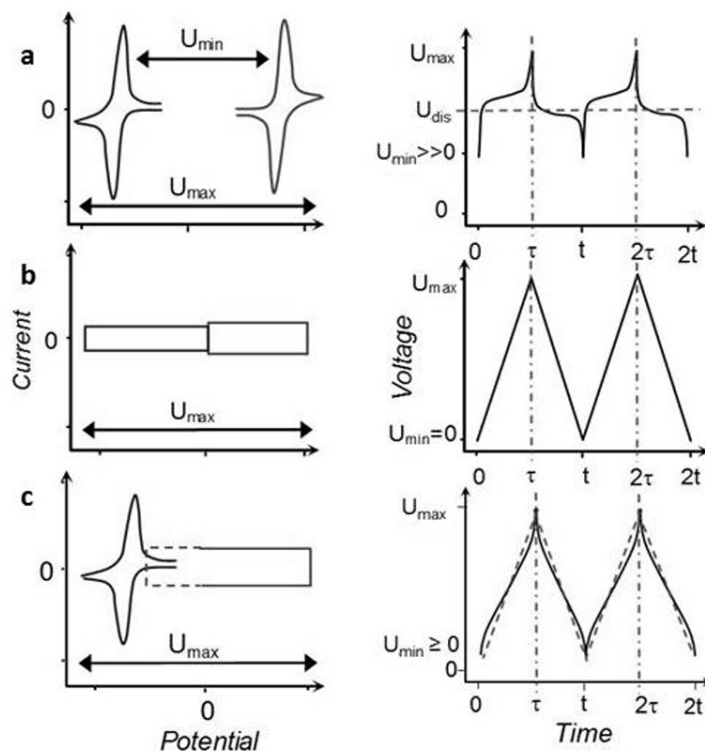


Figure 2. Schematic illustration of the electrochemical characteristics of (a) battery, (b) supercapacitor, and (c) supercapattery represented by (left) the cyclic voltammograms and (right) galvanostatic charging and discharging plots [8] (© The Electrochemical Society, Inc. 2015).

As such in considering the non-linear GCDs which results from the addition of the redox electrolytes, care must be taken in trying to calculate the energy stored, or the $\Delta Q/\Delta U$ ratio. For example in figure 3, the linear GCD (curve A) corresponds to an ideal capacitive response whilst the non-linear GCD (curve B) corresponds to the response of most devices with redox electrolytes. Most literatures characterising the properties of redox electrolytes wrongly misconstrue the $\Delta Q/\Delta U$ ratio obtained from interfaces with DRS as capacitance. Hence, as can be seen in figure 3, this could lead to misleading characterisations of the charge storage properties represented by curve B. A recent report gave detailed clarifications of the issues encountered when trying to explain the charge storage profile of redox electrolytes, and thus suggested that the properties of redox electrolytes should be compared with batteries rather than claiming it as capacitance or pseudocapacitance [8].

The properties of electrodes that could be used for capacitive charge storage includes porous surfaces, surfaces with functional edge sites, and electrodes

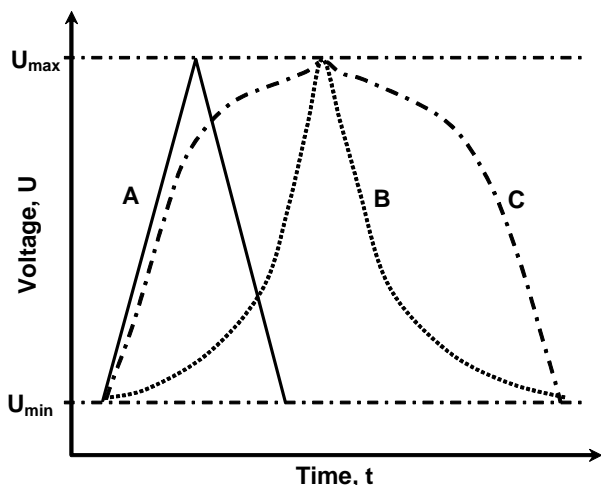


Figure 3. Illustrative comparison of the galvanostatic charging and discharging plots of a conventional SC (plot A, solid line) with a maximum charging voltage, U_{\max} and a minimum discharging voltage, U_{\min} , and the same SC containing a redox electrolyte in which the same redox couple can react on both the positrode and negatrode at the same potential (plot B, dot line), or the redox couple is restricted to react only on either the positrode or negatrode, but not both (plot C, bold dotted line: this has been described in [14]).

that inherently undergo faradaic capacitive reactions. Accordingly, the retention of the redox species *via* various forms of physi-, electro- or chemi-sorption can be used to broadly categorise the enhancement of charge storage at the E/E interface. These categories are:

- i. Dissolved organic redox molecules
- ii. Dissolved redox anionic components
- iii. Dissolved redox cationic components

i. Dissolved organic redox molecules for the enhancement of interfacial charge

The electrochemical properties of some quinonoid compounds have attracted numerous studies in the general literature [21, 22], and the versatility of the quinones have been put into use for applications in SCs [4]. It is generally accepted that the redox reactions of some simple quinonoid compounds, for example hydroquinone (HQ), in aqueous media involve a single step two-electron and two-proton transfer reaction at the electrode [21]. The reversible redox reaction of hydroquinone/benzoquinone in the porous matrix of activated carbon electrodes have been used for enhanced storage [4].

Along these lines, the property of the substituents of hydroquinone i.e. *ortho*-, *meta*-, and *para*-hydroquinone has been studied in acidic media [15]. The poor redox activity of both the *ortho*- and *meta*-substituted hydroquinones at the carbon electrodes observed through three-electrode tests was used to explain their relatively low contribution to charge storage when they were used as redox additives to fabricate SCs with 1 mol/L H_2SO_4 as the electrolyte. This implies that in certain cases the substituent effects could play an important role in the selection of some organic molecules as redox additives.

It has also been shown that interfacial charge at carbon electrodes can be increased by addition of quinones with substituted halides e.g. di-bromo-hydroquinone (DBHQ) in a KOH electrolyte [23]. Experimental findings indicated that the interfacial charge stored was dependent on both the concentrations of the redox additive and the supporting electrolyte. It was also observed that the optimal performance of this redox additive was obtained from an electrolyte of 0.2 mol/L DBHQ and 2 mol/L KOH. The general improvement of charge storage from this additive was attributed to the redox activity of both the quinonoid group and

the bromine substituent [23]. HQ in acidic media has also been used to enhance the charge storage property of a polyaniline-coated curved-graphene oxide (PAn-G) composite. Generally, the recorded increase in interfacial charge was attributed to the redox activity at the electrode surface. However, through impedance measurements it was observed that the charge transfer resistance for the PAn-G in an electrolyte mixed with HQ is greater than the normal H₂SO₄ electrolyte. It was also shown that the charge retention after 10,000 cycles was about 64% (with final capacity values still appreciably greater than the SCs without redox additives), although the electrolyte without additive had over 90% charge retention on comparable cycling. This was attributed to surface-induced effects due to the ionic activities of the redox electrolytes [24].

These investigations involving the use of HQ as redox additive to 1 mol/L H₂SO₄ were extended to include a broad range of electronically conducting polymer (ECP) electrodes such as polyaniline (PAn), polypyrrole (PPy) and poly(3, 4-ethylenedioxythiophene) (PEDOT) [25]. When tested in the two-electrode cell, the most notable performance feature was the appearance of peak-shaped CVs for the PAn cell, but relatively rectangular CVs (and triangular GCDs similar to that in figure 2b) for the cell of PPy or PEDOT with an electrolyte containing HQ. Since in all cases capacitive properties were assumed for all these ECPs, this marked difference in the charge storage profiles of these ECPs operating in electrolytes with redox additives was not clearly elucidated. Moreover, it was shown that the addition of HQ with optimal molarities of 0.3 to 0.4 mol/L in the electrolyte reduces the charge transfer resistance of the devices [25]. Other reports have also described the use of HQ in acidic media with ECP-metal oxide composites. Notably, using a PPy-SnO₂ electrode, the charge storage profile of the HQ/BQ (hydroquinone/benzoquinone) redox couple at the E/E interface was described as a surface-controlled process, leading to an increase in interfacial charge. The charge-discharge profile of the “PPy-SnO₂ electrode/HQ electrolyte” combination also displayed good coulombic efficiency, implying good interfacial kinetics [26].

The redox reaction of the *p*-phenyldiamine/*p*-phenyldiimine couple is a two-electron mechanism

in alkaline media (e.g. KOH), and this has been matched to various properties such as the porosity [13, 27], and surface property [28, 29] of the electrode. The use of *p*-phenyldiamine (PPD) could serve as a good example to highlight some properties of redox additives in practical SCs. Firstly, when dissolved in solutions of neutral aqueous salts, PPD displays relatively slow kinetics [30], whilst in acidic media, it tends to form the protonated salt which on oxidation could lead to an electropolymerisation reaction [31]. Although, this has been adopted for use in co-polymerisation, for example preparation of conducting polymers for energy storage applications, or in the preparation of the polymers of *p*-phenylenediamines [31], such electrochemical properties in acidic media might preclude them from use as dissolved redox species in SCs with acidic electrolytes. This is because reversibility and stability of the dissolved redox species is a vital aspect of their use in practical devices [8]. Accordingly most of all the reports using PPD as the redox additive in SCs have utilised it in either basic solutions, particularly KOH [11, 13, 27, 28] or in aprotic organic electrolytes [32]. Moreover, the solubility of PPD in KOH decreases with increasing concentration of the supporting KOH electrolyte. Accordingly, 2 mol/L KOH has been found to be the optimum supporting electrolyte concentration when PPD is used as the redox additive [13, 33]. Contrastingly, in the application of PPD as redox additive for low-temperature charge capacity enhancement in SCs with MnO₂ electrodes, KOH concentration was increased to 4 mol/L, in order to be able to increase the freezing point of the electrolyte [34].

In general, the electrochemical properties of PPD, particularly its fast redox activity and generally strong surface adsorption of the product of charging implies that when used with mesoporous carbon electrodes, e.g. single-walled carbon-nanotubes (SWCNTs), it displays a large increase in the interfacial charge. Moreover, the devices fabricated with the SWCNT/PPD in the KOH electrolyte displays high charge capacities at relatively high cell voltages [27]. It is also important to state that the use of PPD dissolved in KOH as electrolytes for MnO₂ electrodes [11, 33] reveals how two redox mechanisms (faradaic capacitive in the lattice of the electrode and faradaic non-capacitive from the electrolyte) can provide the increase in interfacial

charge storage for SCs and other related hybrids [3]. Interestingly, in contrast to the meta-hydroquinone additive which displayed a poor interfacial property owing to difficulty in electrochemically oxidising it at the carbon surface, meta-phenyldiamine displayed highly reversible charge transfer kinetics with greatly increased interfacial charge storage [35]. This essentially highlights the importance of the stereochemistry of the DRS when their interfacial properties are to be considered for charge improvement purposes.

A vast number of other organic molecules have been used as DRS in SCs using carbon electrodes. Although the mechanism generally conforms to the generalised description as explained by figure 1, some important observations made in some of these reports are still worth highlighting. By using MWCNTs as electrodes in SCs comprising of methylene-blue (MB) as DRS in 1 mol/L H_2SO_4 , the charge capacity of the electrode was increased markedly. However, in the two-electrode SC test, this increase in charge capacity was obtained at low cell voltage values (< 0.2 V). Also, by adopting the two-electron, two-proton redox reaction of its functional hydroxyl groups, pyrocatechol violet has been used to enhance the charge capacity of AC electrodes [36]. This was carried out by testing pyrocatechol violet as the redox additive in different electrolytes, i.e. 1 mol/L Na_2SO_4 , 1 mol/L H_2SO_4 , and 6 mol/L KOH. Notably, whilst tests in the 3-electrode configuration showed redox peaks in the 1 mol/L Na_2SO_4 and 1 mol/L H_2SO_4 electrolytes, in 6 mol/L KOH there were no identifiable redox peaks, but rather redox waves corresponding to surface-controlled redox reactions at the carbon surface. However, in the two electrode (device) configuration, the CVs for the pyrocatechol violet redox additive in both 1 mol/L H_2SO_4 and 6 mol/L KOH were rectangular i.e. EDL capacitance dominates in the voltage range 0 to 1.0 V. Whereas, for the 1 mol/L Na_2SO_4 supporting electrolyte, two-electrode tests revealed broad peaks [36], essentially pointing out that the charge storage mechanisms in different electrolytes can lead to differences in how the charge capacity of these devices can be characterised in practice.

In KOH solutions, *p*-aminobenzenesulfonate [37] and *p*-nitroaniline [38], both of which can undergo a single proton and single electron transfer reaction,

have been used as DRS. Furthermore, a comparison of the substituent site of the *ortho*-, *meta*-, and *para*-nitroaniline substituents has also shown that in KOH solutions, the redox reaction of *p*-nitrophenol is more effective in acquiring improved interfacial charge storage [39]. It should be pointed out that these redox additives all displayed varying energy efficiency which can be linked to both the surface/morphological properties of the electrodes adopted and also the electrochemical properties of the DRS utilised. Anthraquinone-2,7-disulphonate which undergoes a two-proton, two-electron redox reaction has also been applied to 1 mol/L KNO_3 , and it was shown that the ESR reduced with increasing concentration of the DRS. For example 27.1 ohms for the blank KNO_3 and 15.3 ohms for 0.1 mol/L AQDS in 1 mol/L KNO_3 . Moreover, the energy efficiency was less than 90%, although the charge capacity increase was over 60%.

Organic electrolytes are known to be stable over a wide potential range. Thus, they can be used to fabricate high voltage devices [20]. As such, the charge capacity of SCs using organic electrolytes has also been increased with the use of some organic DRS. Recently, 1,10 phenanthroline was used as DRS in 1.8 mol/L tetraethylammonium tetrafluoroborate ($TEA BF_4$) in polycarbonate. The redox reactions of 1,10 phenanthroline gave a rectangular profile with broad waves corresponding to the oxidation and reduction of phenanthroline, and in 2-electrode device tests the SC containing the phenanthroline showed a rectangular cyclic voltammogram (implying a predominance of EDL capacitance in the device). This device gave over 50% increase in capacitance, although its decrease in capacitance with current density (during galvanostatic charging/discharging) was more rapid than that of the SC without the DRS; still it displayed much higher mass normalised energy and power than the SC without the DRS. More importantly, the device using the DRS displays better cycle stability at higher cell voltages than the device using only the supporting electrolyte [40]. Successful application of *p*-phenyldiamine in 1 mol/L $LiClO_4$ in acetonitrile has also been achieved, confirming a high increase in interfacial charge storage with non-peak-shaped CVs. This is understandable since in aprotic media the electron transfer mechanisms of these organic redox molecules are different from that in aqueous media [32].

ii. Dissolved redox anionic components for enhanced interfacial charge storage

Halides, particularly iodides, have been one of the most important dissolved redox anionic species for increased charge storage in SCs [5]. The highly reversible redox reactions of the I^- anion which could be oxidised to higher polyiodides, e.g. I_3^- and I_5^- , coupled with their strong reversible adsorption at the carbon electrode [5, 41], have made alkali iodides an important DRS for applications in SCs. Basically, on oxidation of the MI ($M = Li, Na, K, Rb$ or Cs), both the reactant and products involving mainly the I_3^- / I^- couple and possibly higher polyiodides would be adsorbed on the electrode, leading to a non-capacitive faradaic (battery-like) charge storage mechanism on the positive electrode. Moreover, the iodides as anions themselves could also contribute to charging the EDLC at the positive electrode.

The interfacial charge stored in the positive electrodes which can be translated to the observed device capacitance also shows some important features that could be linked to the type of metal alkali used. Notably, the electrode capacitance was found to be 203 F/g for NaI and 220 F/g for RbI. This difference was ascribed to the higher polarisation power of Na^+ compared to the larger Rb^+ . Since the same AC was used as positive and negative electrodes in both cases, the larger device capacitance indicates a greater $\Delta Q/\Delta U$ ratio of the positive AC electrode in the RbI electrolyte, considering that $C_{device} = C_+C_-/(C_+ + C_-) = C_-/(1 + C_-/C_+)$ [5, 8]. It is worth mentioning that the claimed capacitance variation of porous carbon electrodes in different iodide containing electrolytes was mainly based on the $\Delta Q/\Delta U$ ratios, disregarding if the CVs or GCDs were capacitive. Future work should re-analyse the results in terms of charge capacity instead of capacitance.

The concentration effects of NaI in SCs have also been used to elucidate the properties of metal halides as DRS for practical applications [42]. Although no linear correlation was found between an increase in NaI concentration and the performance of the devices, 2 mol/L performed better than 5 mol/L [42]. Interestingly, a high concentration of 6 mol/L KI was recently used as DRS for carbon-beads electrode, and the device showed high rate cycle stability after 10,000 cycles [18]. The influence of the concentration

of KI as additives to a 1 mol/L Li_2SO_4 electrolyte used in fabricating asymmetric SCs comprising of the composite of ZrO_2 -MWCNT as positive electrode and WO_3 -MWCNT as negative electrode has also been reported [43]. It was shown that increasing the concentration of KI from 7.5 to 30×10^{-3} mol/L dramatically affects the charge storage profile of the device. For example at 7.5 and 15×10^{-3} mol/L KI the CV of the device was rectangular; however at 30×10^{-3} mol/L KI, the CV of the device develops sharp peaks. Moreover, the capacitance of the device tested at a current load of 1 A/g was 198 F/g for the device with 7.5×10^{-3} mol/L KI and 96 F/g for the device using Li_2SO_4 without the redox additive, and the cell operated at an optimal voltage of 2.2 V. This essentially shows that paying close attention to the concentration of the redox electrolytes as additives can indeed lead to improved devices, particularly in asymmetrical SC designs [43]. It is important to point out that although capacitance was not normalised for the amount of redox additive, the capacitance increase at such small addition of DRS is appreciable, and in comparison with other devices that utilise much more higher concentration of additives, this device arrangement seems to display optimal performance metrics.

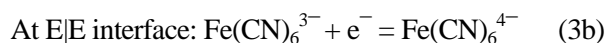
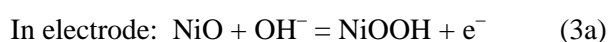
Using LiI as additive to a solution of Li_2SO_4 and methanol in a symmetric SC with AC electrodes, the self-discharge properties and the low temperature properties were investigated. It was observed that the presence of LiI in the electrolyte helped improve the charge capacity at a low temperature of $-40^\circ C$ [44]. The advantageous properties of the mesoporous structure of MWCNTs when they were used as additives to AC electrodes were also described when 1 mol/L KI was used as DRS in SCs. This improvement in charge storage properties was attributed to the improved ionic conductivity due to the presence of mesopores which can benefit to the transport of the iodide and polyiodide anions [17].

The $Fe(CN)_6^{3-}/Fe(CN)_6^{4-}$ couple is a typical example for describing redox reactions in the literature. Accordingly, the exemplary electrochemical property of this couple has been adopted as DRS for SC applications. Carbon electrodes that have been used to test the suitability of this couple for improving charge storage in SCs include graphene paper [45], vertically aligned carbon nanotubes (VACNTs) [46],

and AC [47]. Since the desirable reversibility of the $\text{Fe}(\text{CN})_6^{3-}/\text{Fe}(\text{CN})_6^{4-}$ redox reaction is well known, another important property that should be considered is the adsorption of these redox anions at the positive electrode. In practice, it has been shown that although the electrostatic attraction of these redox anions to the positive carbon electrode interface is relatively strong, the adsorption of these anions at the interface is still quite low. A recent spectroscopic investigation of the adsorption of the $\text{Fe}(\text{CN})_6^{3-}/\text{Fe}(\text{CN})_6^{4-}$ couple at AC showed low adsorption for the oxidation product. This property was used to explain the high rate of self-discharge in devices using $\text{Fe}(\text{CN})_6^{3-}/\text{Fe}(\text{CN})_6^{4-}$ as DRS. In contrast, devices using the I_3^-/I^- couple which showed high adsorption at the carbon surface displayed self-discharge properties that were 100 times slower than that of devices using the $\text{Fe}(\text{CN})_6^{3-}/\text{Fe}(\text{CN})_6^{4-}$ as DRS [41]. This high rate of self-discharge is the reason why ion-selective separator membrane was used to improve the practical device performance of SCs using the $\text{Fe}(\text{CN})_6^{3-}/\text{Fe}(\text{CN})_6^{4-}$ couple as DRS [47]. A detailed description of the general design of practical devices using DRS is given in section 3.

Despite the low adsorption leading to high rate of self-discharge of the $\text{Fe}(\text{CN})_6^{3-}/\text{Fe}(\text{CN})_6^{4-}$ couple as DRS, a large improvement in the interfacial charge of graphene paper has been reported, and this charge capacity increase showed a strong dependence on the concentration of the $\text{K}_3\text{Fe}(\text{CN})_6^{3-}$ redox additive in 1 mol/L Na_2SO_4 [45]. Also, by using VACNT as the electrode material, it was shown that the redox activity of the $\text{Fe}(\text{CN})_6^{3-}/\text{Fe}(\text{CN})_6^{4-}$ couple was confined in the macropores of the VACNT, leading to an electrode-confined thin-layer effect characterised by high-rate and low-diffusion charge storage in the porous structure of the electrode material. This E/E interface displayed high stability after 5000 cycles, whilst also maintaining its coulombic efficiency of 97% throughout the cycling period [46]. In another investigation, equimolar proportions of the $\text{K}_4\text{Fe}(\text{CN})_6$ and $\text{K}_3\text{Fe}(\text{CN})_6$ redox additives in alkaline KOH electrolyte were used to increase the interfacial charge of a NiO electrode. Due to the increase in charge capacity, the electrode also showed improved charge storage properties at a low temperature of -20°C [11].

Additionally, the $\text{Fe}(\text{CN})_6^{3-}/\text{Fe}(\text{CN})_6^{4-}$ couple has been applied to improve the interfacial charge storage of transition metal hydroxide electrodes such as $\text{Co}(\text{OH})_2$ -graphene nanosheet [48], Co-Al double hydroxide [49], and ECP electrodes, for example polyaniline [50]. It should be pointed out that the use of redox electrolytes with redox electrodes exemplifies dual interfacial redox mechanisms occurring in the lattice of the electrode and in the electrolyte. This is illustrated by equations 3a and 3b, which show the electrode and electrolyte redox mechanisms at the NiO/DRS interface, respectively [11].



Moreover, only interfacial properties of these combinations of transition metal hydroxide electrode and DRS have been described thus far, and the performance of practical devices using such combined storage mechanisms has not yet been given detailed treatments. Strategies that could be used to enhance the charge storage properties for such redox-electrode and redox electrolyte combinations would be broadly described in section 4. It is also important to point out that the MoO_4^{2-} anion obtained from using Na_2MoO_4 as DRS was shown to improve the capacitance of a symmetric EDL capacitor with AC electrode from 51 F/g in 1 mol/L Li_2SO_4 to 65 F/g in 1 mol/L $\text{Li}_2\text{SO}_4 + 0.1$ mol/L Na_2MoO_4 (calculated based on rectangular CVs). The optimal cell voltage of this device was 1.6 V. The Na_2MoO_4 redox additive also increased the passivation of the stainless steel current collector, thereby reducing its susceptibility to pitting corrosion due to attack from the SO_4^{2-} ion [51].

iii. Dissolved redox cationic components for enhanced interfacial charge storage

When a positive electrode is functionalised with cation affinitive groups, electroactive cations from the electrolyte could be chemically adsorbed at these positive electrodes, even though cations are not electrostatically attractive to positive electrodes. Since carbon atoms at the edge sites are more reactive than the internal carbon atoms, these edge sites could readily become oxidised (or stabilised) thereby forming oxygen-containing groups, e.g. $-\text{OH}$ and $-\text{COOH}$, etc. These functional groups

which can be deprotonated to become negatively charged would then have a high cation affinity. On the other hand, irrespective of deprotonation, the highly electronegative oxygen (and also nitrogen, sulphur and halogen) atoms can still offer some affinity to metal cations [8].

Examples of this mechanism include “(+) $\text{AC} \mid \text{CuSO}_4 - \text{FeSO}_4 - \text{H}_2\text{SO}_4$ ” [6], “(+) $\text{functionalised carbon surface} \mid \text{CuCl}_2 - \text{HNO}_3$ ” [10], and “(+) $\text{Graphene-felt} \mid \text{Ce}^{3+} - \text{H}_2\text{SO}_4$ ” [52]. Brief descriptions of these mechanisms for charge storage at the stated interfaces are presented forthwith. When CuSO_4 and FeSO_4 were used as mixed redox additives in H_2SO_4 , the charge storage property was observed to be related to the concentrations of the Fe^{2+} and Cu^{2+} ions, and also with the porosity of the carbon electrode. It was thus shown that using the CuSO_4 electrolyte alone as additive gave a poor reversibility. However, on mixing with FeSO_4 , improved charge storage properties was observed. In general, the reaction mechanism for this improved charge storage is mainly due to the accessibility of the Cu^{2+} and Fe^{3+} ions to the surface oxy-groups of the carbon electrode [6]. The mixture of CuCl_2 and HNO_3 as electrolyte for porous carbon microsphere (PCM) electrode resulted in large interfacial charge storage. This was attributed to the adsorption of Cu^{2+} on the surface carbonyl groups to form a reversibly adsorbed layer of CuCl_2 on the surface of the PCM electrode. It was also important to locate an optimal potential range across the interface in order to prevent the irreversible deposition of Cu [10].

The use of an electrode material that provides a high overpotential for the redox reaction of the $\text{Ce}^{4+}/\text{Ce}^{3+}$ in aqueous (acidic) media has been shown to be greatly dependent on the surface property of the graphene-felt electrode used [52]. This is because when the reaction in equation 4 takes place in acidic media, e.g. 1 mol/L H_2SO_4 , the standard electrode potential (SEP) for the reaction is 1.44 V vs NHE. Thus if an electrolyte, e.g. $\text{Ce}_2(\text{SO}_4)_3$ dissolved in 1 mol/L H_2SO_4 is used as the source of the $\text{Ce}^{4+}/\text{Ce}^{3+}$ couple, the redox reaction cannot occur within the stable operating potential of water. However, if an electrode with a higher overpotential for the evolution of oxygen is employed, then this redox reaction can be accommodated without electrolyte decomposition thus leading to improved charge storage at more

positive potentials. This reasoning has been used to develop an asymmetric SC with AC as the negative electrode, and modified graphite felt as the positive electrode. The resulting device was operated at an optimal cell voltage of 1.5 V (with specific energy of about 13.8 Wh/kg) [52].



It is also important to mention that the $\text{Fe}^{3+}/\text{Fe}^{2+}$ couple (in 1 mol/L H_2SO_4) has been used to enhance the interfacial charge properties of the polyaniline- SnO_2 composite electrode, and the increased interfacial charge was relatively stable after 2000 galvanostatic charge-discharge cycles at 1 A/g [53]. Also, the $\text{Cu}^{2+}/\text{Cu}^+$ couple (in 1 mol/L H_2SO_4) was used to enhance the interfacial charge of the PAN electrode, giving rise to improved charge capacity. However, due to the well-known complicated heterogeneous reaction kinetics involving the reduction-caused Cu deposit on the electrode surface, the rate property of the electrode was relatively poor [54].

4. Design of supercapacitors with dissolved redox species

For the application of dissolved redox species (DRS) in practical devices, some properties such as the solubility, pH and temperature can play important roles in affecting the charge storage mechanism at the interface. Also of importance is the concentration of DRS/supporting electrolyte, or the concentration of the electrolyte if it is inherently redox active. Moreover, two other important properties of DRS that should be taken into consideration in the design of devices are (1) the adsorption of the products of the redox reaction on the electrode surface (which affects the self-discharge of the device), and (2) the electrode potential of the redox additive employed (which affects the voltage at which the increased charge capacity is obtained at the device-level).

Figure 4 (a and b) gives a generalised and schematic description of the design of an electrochemical energy store, for instance a SC or battery. Figure 4a corresponds to the device in the charging mode and figure 4b to the discharging mode. In the most general case, this charge storage device can comprise of two non-mixing electrolytes namely the negalyte

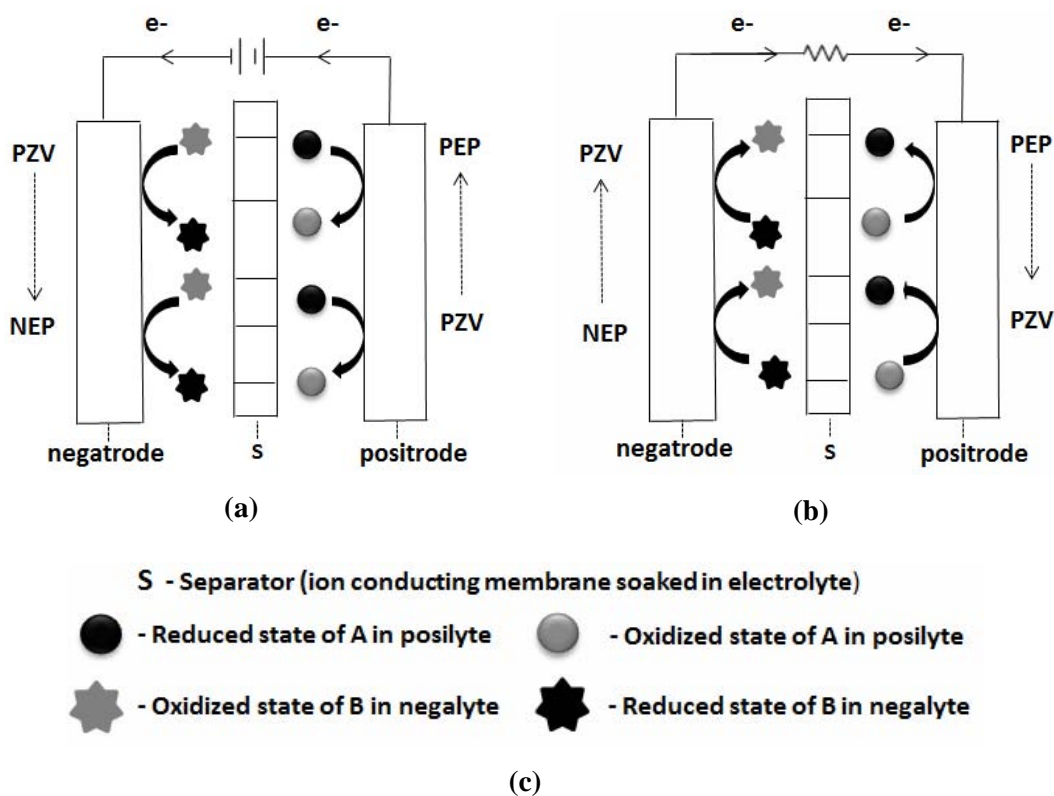


Figure 4. Generalised diagrams of an electrochemical storage device (a) under charging and (b) under discharging conditions. (c) Explanations to symbols in (a) and (b). PEP and NEP are the positive and negative electrode potentials, respectively, measured at the maximum cell voltage. PZV (point of zero voltage), is the equipotential of the positive and negative electrodes at zero cell voltage.

which is the electrolyte at the negative electrode (negatrod) and the posilyte which is the electrolyte at the positive electrode (positrod). The terms positrod, negatrod, posilyte, and negalyte are used in place of the terms of cathode, anode, catholyte and anolyte, respectively. The former terms were recently introduced as a means of avoiding the confusion that inevitably arises when the latter terms are used in fundamentally describing the components of electrochemical energy stores [2]. For example, it is a fact that a positrod is a cathode in discharging but an anode in charging. Similar situations apply to the use of negatrod, posilyte and negalyte. In figure 4, S is a separator membrane, and it could either be an ion-exchange membrane (IEM) which allows the passage of specific ions, whilst blocking the passage of others, e.g. Nafion membrane, or a normal porous separator membrane, e.g. glass-fibre paper. A number of scenarios would now be used to describe various features of this configuration in practice.

When this device is adopted exactly as is shown (i.e. the separator membrane is able to prevent electrolyte mixing), on charging, the DRS in the posilyte is oxidised whilst the DRS in the negalyte is reduced (Figure 4a). On discharging the DRS in the posilyte is reduced and the DRS in the negalyte is oxidised (Figure 4b). If the separator completely compartmentalises these redox species but allows ionic conduction of protons, cations or anions, whilst been able to stop the cross-diffusion of the products of the electrode reactions, there would be limited self-discharge of such a cell under open circuit conditions. (Note that open circuit conditions correspond to a removal of the load in figure 4b). Such a design strategy could result in optimum devices.

Such a configuration was applied in a device comprising of $(-)\text{AC} \mid \text{VOSO}_4 \parallel \text{KI} \mid \text{AC}(+)$, which makes use of the redox reactions of the $\text{VO}_2^{2+}/\text{VO}_2^+$ couple in the negalyte and the I_3^-/I^- couple in the

posilyte. The separator denoted by || was a proton exchange membrane (Nafion 117). This device showed improved charge capacities, with the positrode being characterised by the reaction mechanism resulting in strong adsorption of the I_3^-/I^- couple, whilst the VO^{2+} can transfer electrons to the negatrode along the $-COOVO^+$ bond between the oxy-group and VO^{2+} ion in the negatrode [55].

It is interesting to note that a related adaptation of this concept has been applied to Li-ion battery research. In this case the configuration is $(-)\text{Li-metal} | \text{organic electrolyte} || \text{LiI-KI-I}_2 | \text{AC}(+)$, where the organic electrolyte (negalyte) is 1 mol/L LiPF_6 in ethylene carbonate/dimethyl carbonate, and the separator (||) is the glass ceramic separator LATP (i.e. $\text{Li}_2\text{O-Al}_2\text{O}_3\text{-P}_2\text{O}_5$) which allows the passage of only Li^+ , but blocks the passage of other solution components. The resulting device displayed charge capacity approaching 98% of the theoretical capacity of the aqueous posilyte. It should be noted that the charge capacity reported was normalised to the total mass of the active species in the posilyte since the investigators could measure the mass of posilyte confined in the positive portion of their cylindrical cell design. Also, the theoretical electrode capacity was normalised based on all active components, leading to reliably calculated performance metrics [56]. In the design of this hybrid device which uses an aqueous DRS/carbon positrode, it should be noted that the mechanism of charge storage is due to the Li^+/Li redox mechanism of the negatrode/negalyte and the I_3^-/I^- redox mechanism of the DRS in the posilyte. As such it made use of the good interfacial properties of the " $I_3^-/I^- | \text{AC}$ " interface, leading to a high-energy prototype device with a coulombic efficiency of over 97% [56].

In the case where the posilyte and the negalyte are the same as in a conventional cell, but with the electrolyte consisting of a DRS, for example hydroquinone dissolved in H_2SO_4 [4, 57], or $\text{K}_3\text{Fe}(\text{CN})_6$ dissolved in Na_2SO_4 [47], then one can visualise the main redox mechanism as the one occurring at the positrode/posilyte interface. Accordingly, if the DRS is assumed to be hydroquinone, then the reaction would involve the oxidation of hydroquinone into benzoquinone at the positrode according to equation 5 (where HQ is hydroquinone and BQ is benzoquinone):



From equation 5, it can be appreciated that although the product of the charged species, i.e. BQ, could adsorb on the AC positrode, it might still diffuse into the electrolyte and then migrate to the negatrode. Accordingly, if in figure 4b we assume that there is no load across the terminals (i.e. at open circuit state) then the BQ that diffuses into the negalyte portion of the cell can then be reduced at the negatrode, and this would in turn positively shift the potential of the negatrode, thus reducing the overall voltage of the cell.

This mechanism, known as redox shuttling, accounts for the high rate of self-discharge that some practical devices using DRS suffer from, as has been rigorously described in [57]. Thus, if the separator S is an ion-exchange membrane (e.g. a proton exchange membrane) which could impede the movement of BQ into the negalyte compartment of the cell, whilst allowing the transport of the H^+ ions, then the self-discharge rate can be reduced. This strategy has been adopted to mitigate the self-discharge of SCs using graphene-hydrogel electrodes with a DRS of 0.4 mol/L HQ dissolved in 1 mol/L H_2SO_4 . The self-discharge rate was markedly reduced in the device using the Nafion membrane in comparison with the device that used conventional polymeric separators [57]. Accordingly, by making use of an ion-exchange membrane, a SC with AC electrodes using $\text{K}_3\text{Fe}(\text{CN})_6$ as DRS in 1 mol/L Na_2SO_4 showed improved charge capacity. A high cell voltage of 1.8 V was recorded for this cell. Also, the performance of EDLCs (without the DRS) using either the glass-fibre paper or IEM was similar, although the ESR of the device using the IEM increased with increasing the IEM thickness. Furthermore, after 15000 cycles this report also demonstrated that there was no marked degradation of the IEM. Thus, apart from the slight difference in power response (ion transport in IEMs is slower compared to the conventional glass-fibre or filter paper), the charge storage profile of these two types of separators are identical. Moreover, the use of the IEM greatly improved the charge storage properties of the device with the DRS, whilst DRS-containing devices using conventional porous separators showed a comparatively poor performance due to redox shuttling [47].

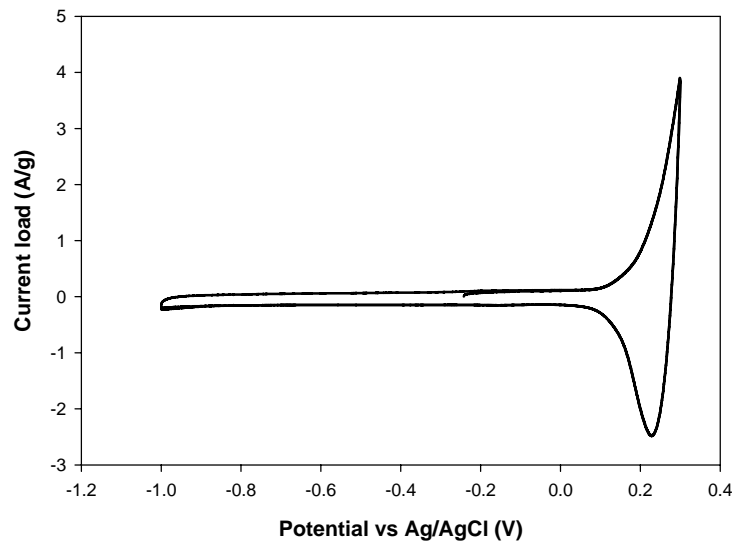
Another important property for consideration in the selection of DRS for practical applications is the standard electrode potential of the redox reaction of the DRS. This is important because in certain cases when the positive potential of the redox reaction is relatively less positive, the charge capacity increase of the resulting device would occur at low voltage values, which is of little use in terms of energy storage capacity. KI as the redox additive can be used to explain this point. Figure 5a shows the CV of an AC electrode in a 2 mol/L KI as redox electrolyte, whilst figure 5b shows the CV of the SC with two AC electrodes and 2 mol/L KI electrolyte. As seen from figure 5b, the high charge capacity from the 2 mol/L KI is obtained at low voltage values, due to the less positive standard electrode potential of the I_3^-/I^- redox reaction. Also, curve B in figure 3, is an illustration of the likely GCD curve when couples with less positive electrode potentials e.g. I_3^-/I^- are used as the positive in SCs. Moreover, the selection of DRS in practice is constrained by the appropriate pH at which the thermodynamics and kinetics of the redox reaction would be favourable, and also by the stability of aqueous solutions at different pH values. Consequently, most of the reports using DRS have actually made use of the common redox additives, for example HQ [4] and also $FeSO_4$ and $CuSO_4$ [6] in acidic electrolytes, PPD in alkaline media [35], and KI in neutral solutions [5], within the bounds of the thermodynamic restrictions. This is one of the reasons why device engineering as described in figure 4 is important when using DRS in practical devices.

In a recently reported approach, the electrolyte comprising mixed $VOSO_4$ and $SnSO_4$ in 0.1 mol/L H_2SO_4 was used as the DRS [9]. In this investigation, the electrolyte composition was not separated into negalyte or posilyte, although an anion-exchange membrane was used as the separator to prevent the redox shuttling of the active species. Accordingly, the designed cell was able to confine the redox reaction of VO^{2+}/VO_2^+ to the positive. Also, the redox reactions of VO^{2+}/V^{3+} , V^{3+}/V^{5+} and Sn/Sn^{n+} (i.e. deposition of tin on the surface of the AC during charging of the cell, and the dissolution of the deposited tin into mainly Sn^{2+} and possibly Sn^{4+} during the discharging of the cell) were confined to the negative. Post-mortem analyses of the electrodes

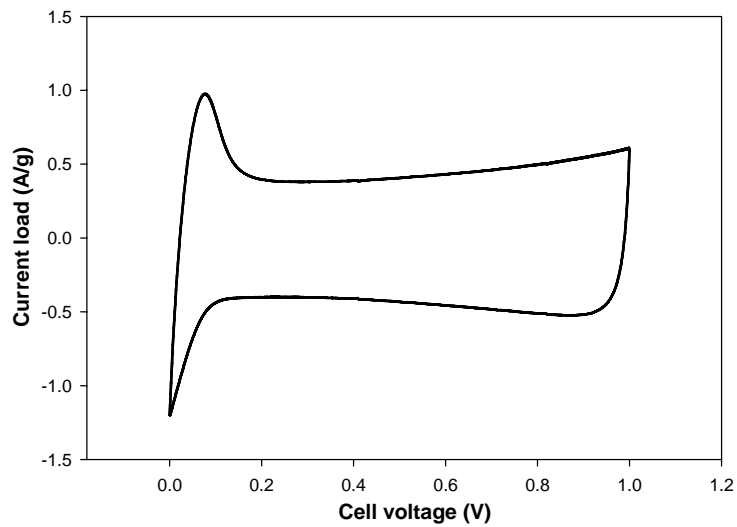
used in these cells also pointed out the possibility that these redox reactions mainly occurred within the porous structure of the AC electrodes utilised. This arrangement resulted in a battery-like storage which operated at an optimal cell voltage of 1.4 V and displayed relatively high-power performance during galvanostatic charge-discharge cycles [9].

The ability of well-chosen membranes (ion-exchange or otherwise) to physically separate the two different electrolytes i.e. the negalyte and posilyte, in addition to being used to confine the redox mechanism occurring at both electrodes without shuttling, can also be applied in practice to increase the maximum cell voltage of devices using DRS. It has been explained that using the KI DRS in an unseparated cell can result in devices with high charge capacity at low cell voltage (see curve B in figure 3, and Figure 5a and b). However, by separating KI in the posilyte from KOH in the negalyte, it has been shown that the cell voltage of these devices can be extended from about 1 V in the case of the unseparated symmetric cell using KI, to 1.5 V for the cell with the configuration of “(-)AC | KOH || KI | AC(+)”. This cell arrangement makes use of the high overpotential for hydrogen evolution on the AC negative in alkaline media, to extend the capacitive potential range of the negative (without DRS in the negalyte), thus increasing the maximum cell voltage of the device [14]. This can be seen in figure 6 (a and b). Also, the GCD curve B in figure 3 which corresponds to the CV in figure 6b, is an illustration of a SC using DRS in which the increased charge capacity is obtained at high voltage values (Note that curves B and C are features of devices which have been described as superbatteries, because the battery-like properties of the devices dominate over the inherent supercapacitive properties of one or both of the electrodes used [2, 8]). It should also be pointed out that for the cell (-)AC | KOH || KI | AC(+), the separator (||) does not need to be an ion exchange membrane. Moreover, it must be able to prevent the mixing of the electrolytes. Accordingly, devices of this sort are designed in such a way that the positive and negative do not have excess posilyte or negalyte, respectively [14].

Similarly, by designing a cell comprising of a high pH negalyte and acidic posilyte i.e. “(-)AC | $MgSO_4 + KOH$ || $KI + H_2SO_4$ | AC(+)”, cells with



(a)



(b)

Figure 5. Cyclic voltammogram at 5 mV/s of (a) an AC electrode in 2 mol/L KI electrolyte; (b) a SC with AC electrodes and 2 mol/L KI electrolyte.

maximum voltage of about 1.8 V have been demonstrated. It was shown that their performance exceeded that of the cell with mixed MgSO_4/KI electrolyte [58]. It is also important to point out that this use of dual electrolytes has been adopted as a means of increasing the maximum cell voltage of conventional SC devices (i.e. without any dissolved redox species). Notably, the configuration “(-)AC | KOH || LiNO_3 | AC(+)”

has been used to design cells with maximum operating voltages of 2.2 V [59]. This implies that by confining the electrolytes to particular electrodes, the full stable potential window of the E/E interface can be reached, leading to increased maximum cell voltage for the device. These aforementioned device engineering approaches are indeed promising, but it should be pointed out that their commercial adoption might be challenging.

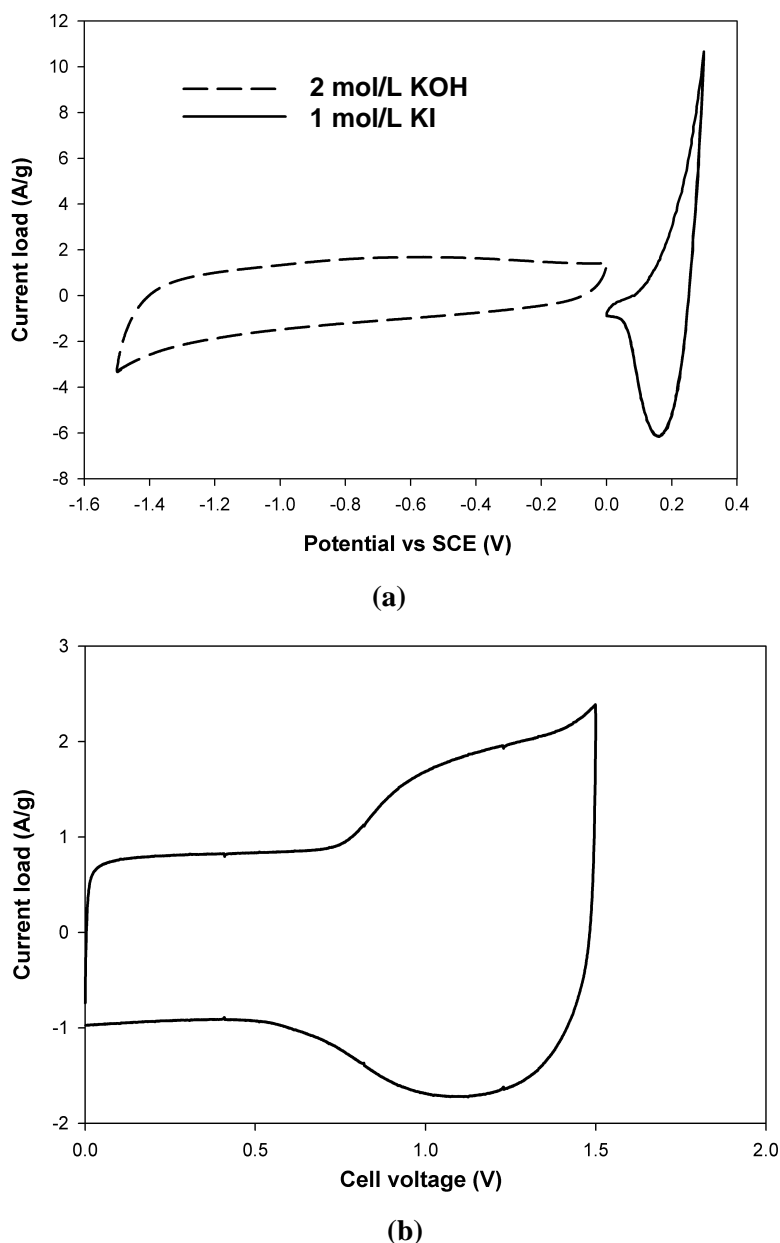


Figure 6. Cyclic voltammogram at 10 mV/s showing (a) electrode potential of dual electrolyte cell comprising of 2 mol/L KOH (negalyte) and 1 mol/L KI (posilyte); (b) cell comprising of 1 mol/L KI (posilyte) and 2 mol/L KOH (negalyte).

In a bid to design devices with high maximum cell voltage using DRS but circumventing the use of (relatively expensive) ion-exchange membranes, the mixed electrolyte comprising of KBr and methyl-viologen-dichloride ($MVCl_2$) was used in an SC device with carbon electrodes. This device exploited the strong adsorption of the product of the reduction of the methyl-viologen cation and

oxidation of Br^- at the negatrod and positrod, respectively. The resulting device operated at a maximum cell voltage of 1.4 V with a low rate of self-discharge [41]. It has also been shown that some redox electrolytes which undergo interfacial chemical reactions leading to strongly adsorbed complexes on the carbon surface can result in devices that display improved charge capacity and

reduced rate of self-discharge. This has been applied when the electrolyte of mixed heptyl-viologen and NaBr was used with AC electrodes. This device made use of the surface-adsorbed complexes reversibly formed and dissolved during charging and discharging, respectively. On the positrode Br^- was oxidised to Br_3^- which then reacted with the HV^{2+} to form the adsorbed $[\text{HV}^{2+} \cdot 2\text{Br}_3^-]_{\text{ads}}$ complex. On the negatrode HV^{2+} was reduced to HV^+ which then reacted with the Br^- to produce the adsorbed $[\text{HV}^+ \cdot \text{Br}^-]_{\text{ads}}$ complex. The reverse of this reaction occurred during discharging when the surface-adsorbed complexes both dissolved. Equation 6 (a and b) describes this process, where the forward reaction corresponds to charging, and the reverse reaction to discharging the cell [12].



Other noteworthy applications of DRS to practical devices include the use of 1-ethyl-3-methylimidazolium bromide that was dissolved in 1-ethyl-3-methylimidazolium tetrafluoroborate, leading to a highly stable device after 10,000 charging-discharging cycles [60]. Another recent report also showed the use of redox-active ionic liquids to improve the interfacial charge of AC electrodes [61].

With increasing attempts at developing flexible supercapacitors, the use of polymer electrolytes has been on a rise [62]. Briefly, the polymer electrolyte comprises of the binder material (e.g. PVA) and the electrolyte (H_2SO_4), and it is placed in between the positrode and negatrode, making the polymeric electrolyte both separator and electrolyte [63]. Essentially, with the redox electrolyte added into the polymer electrolyte composition, the so-called redox-polymer electrolyte is formed. Some examples include PVA- H_2SO_4 -hydroquinone [62], PVA-KOH-KI [63] and PVA- H_2SO_4 -alizarine red S [64]. In general, some of these investigations have shown that the conductivity of the gel-polymer electrolyte increases with increase in concentration of the redox additive. This is mainly attributed to improved charge transport on the application of the ionic additive. However at much higher concentrations, conductivity reduces due to migration effects or phase separation [64]. In general, this increase in conductivity of gel polymer electrolyte

with the incorporation of redox additives have been linked to improved rate kinetics from impedance spectroscopic investigations [65]. Due to the inherent properties of these redox polymer electrolytes, the energy efficiency in some cases is low [66], although some of these devices are promising [64].

5. Concluding remarks

The use of electrolytes containing dissolved redox species (DRS) has been described as an important means of enhancing the storage performance of SCs. The research trends are geared towards understanding the role of the surface properties of electrodes and their interactions with the redox electrolytes. These include the modification or synthesis of electrolytes to obtain E/E interfaces that display improved charge storage properties [12, 23], and the use of various types of ion-exchange membranes [9, 47], or optimised polymeric separator membranes [59].

Essentially, some practical aspects of research into the use of DRS would closely depend on the developments of membrane technologies that are of use in other related electrochemical energy storage systems, for example redox flow batteries [67]. The broad array of synthesis methods to produce electrode materials displaying a wide variety of morphology, porosity, surface properties etc. can be used in matching suitable redox electrolyte for improved interfacial charge storage [68]. Also, investigations on the properties of redox ionic liquids [61] and the use of redox additives in polymeric electrolytes [65] are important aspects of research on DRS. Furthermore, the use of simulation tools to understand surface adsorption of quinonoid groups on carbon surface [69], is also important to the fundamental studies and applications of DRS.

In general, it is important to state that a major motivation for investigating the application of DRS in SCs is because of the facile approach which it promises. For example, one may consider the simplified production line of a commercial SC shown in figure 7. With clearly identified redox additives for improved charge capacity at the carbon electrode, it is easy to appreciate that such an adoption of DRS can be integrated into the production line at P2, with minimum adjustment

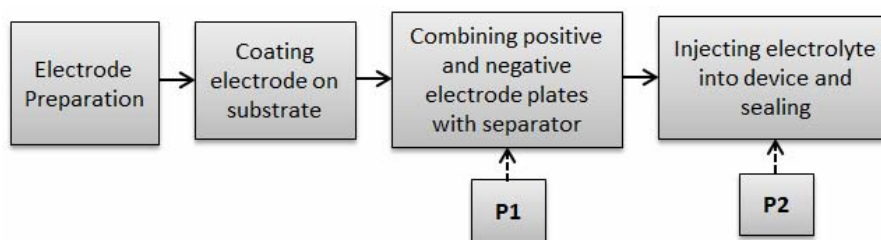


Figure 7. Simplified illustration of the production process of a SC. P1 corresponds to the point where technologies such as using special membranes or dual electrolytes have to be included into the process. P2 corresponds to the point where dissolved redox species can just be added to conventional SC electrolyte.

to the existing manufacturing technologies [9]. On the other hand, the use of novel cell designs which could involve adopting specialised separators (integration from P1) or the use of dual electrolytes would require significant adjustments to currently existing manufacturing technologies of SC devices [59].

It is also important to point out that the grafting of these redox species into carbon electrode materials [70] or ECPs [54] is another important research area, although these methods also face a number of challenges such as passivation after long cycles [54], instability/solubility of the electrodes [70] etc. The low self-discharge rates of some of these devices with grafted redox species compared to when the redox species is dissolved in solution [71] implies that grafting of these species into the electrode is also promising. Moreover, it is important to note that grafting redox additives to the electrode structure is not aimed at replacing the use of DRS in practice. This is because the targets of these two research aspects are different. For example, whilst at its most basics, the use of DRS targets P2 (i.e. simple modification of the existing electrolytes using current technology), the use of electrode grafting would have to affect the supply side of the carbon (or other electrode) materials. Moreover, most SC manufacturers obtain their activated carbon electrode materials from vendors [72]. Thus, electrode grafting would have a slightly challenging commercial entry-point compared to the simple modification of electrolytes for improved charge storage which the use of DRS promises.

ACKNOWLEDGMENTS

The authors thank the Ningbo Municipal Government for financial support *via* the 3315 Plan and the

IAMET Special Fund, 2014A35001-1, and also the International Doctoral Innovation Centre of the University of Nottingham Ningbo China for awarding a PhD Scholarship to B.A.

CONFLICT OF INTEREST STATEMENT

The authors declare no conflict of interest.

REFERENCES

1. Dunn, B., Kamath, H. and Tarascon, J-M. 2011, *Science*, 334, 928.
2. Chen, G. Z. 2017, *Int. Mater. Rev.*, 62, 173.
3. Guan, L., Yu, L. and Chen, G. Z. 2016, *Electrochim. Acta*, 206, 464.
4. Roldan, S., Granda, M., Menendez, R., Santamaria, R. and Blanco, C. 2011, *J. Phys. Chem.*, 115, 17606.
5. Lota, G., Fic, K. and Frackowiak, E. 2011, *Electrochem. Commun.*, 12, 38.
6. Li, Q., Li, K., Sun, C. and Li, Y. 2007 *J. Electroanal. Chem.*, 611, 43.
7. Senthilkumar, S. T., Selvan, R. K. and Melo, J. S. 2013, *J. Mater. Chem. A*, 1, 12386.
8. Akinwolemiwa, B., Peng, C. and Chen, G. Z. 2015, *J. Electrochem. Soc.*, 162, A5054.
9. Lee, J., Krüner, B., Tolosa, A., Sathyamoorthi, S., Kim, D., Choudhury, S., Seo, K.-H. and Presser, V. 2016, *Energy Environ. Sci.*, 9, 3392.
10. Mai, L-Q., Minhas-Khan, A., Tian, X., Hercule, K. M., Zhao, Y-L., Lin, X. and Xu, X. 2013, *Nat. Commun.*, 4, 2923.
11. Su, L., Gong, L. and Zhao, Y. 2014 *Phys. Chem. Chem. Phys.*, 16, 681.
12. Evanko, B., Yoo, S. J., Chun, S-E., Wang, X., Ji, X., Boettcher, S. W. and Stucky, G. D. 2016, *J. Am. Chem. Soc.*, 138, 9373.

13. Wu, J., Yu, H., Fan, L., Luo, G., Lin, J. and Huang, M. 2012, *J. Mater. Chem.*, 22, 19025.
14. Fic, K., Meller, M. and Frackowiak, E. 2015, *J. Electrochem. Soc.*, 162, A5140.
15. Frackowiack, E., Meller, M., Gastol, D. and Fic, K. 2014, *Faraday Discuss.*, 172, 179.
16. Senthilkumar, S. T., Selvan, R. K., Lee, Y. S. and Melo, J. S. 2013, *J. Mater. Chem. A.*, 1, 1086.
17. Meller, M., Menzel, J., Fic, K., Gastol, D. and Frackowiak, E. 2014, *Solid State Ionics*, 265, 61.
18. Krüner, B., Lee, J., Jackel, N., Tolosa, A. and Presser, V. 2016, *ACS Appl. Mater. Interfaces*, 8, 9104.
19. Chabi, S., Peng, C., Hu, D. and Zhu, Y. 2014, *Adv. Mater.*, 26, 2440.
20. Conway, B. E. 1999, *Electrochemical Supercapacitors: Scientific fundamentals and technological applications*, Kluwer-Plenum, New York.
21. Quan, M., Sanchez, D., Wasylkiw, M. F. and Smith, D. K. 2007, *J. Am. Chem. Soc.*, 129, 12847.
22. Gupta, N. and Linschitz, H. 1997, *J. Am. Chem. Soc.*, 119, 6384.
23. Gastol, D., Walkowiak, J., Fic, K. and Frackowiak, E. 2016, *J. Power Sources*, 326, 587.
24. Chen, W., Rakhi, R. B. and Alshareef, H. N. 2013, *Nanoscale*, 5, 4134.
25. Chen, W., Xia, C., Rakhi, R. B. and Alshareef, H. N. 2014, *J. Power Sources*, 267, 521.
26. Zhu, Y., Liu, E., Luo, Z., Hu, T., Liu, T., Li, Z. and Zhao, Q. 2014, *Electrochim. Acta*, 118, 106.
27. Yu, H., Wu, J., Lin, J., Fan, L., Huang, M., Lin, Y., Li, Y., Yu, F. and Qiu, Z. 2013, *ChemPhysChem*, 14, 394.
28. Zhang, Z. J., Zhu, Y. Q., Chen, X. Y. and Cao, Y. 2015, *Electrochim. Acta*, 176, 941.
29. Nie, Y. F., Wang, Q., Yi, H. T., Chen, X. Y. and Zhang, Z. J. 2015, *RSC Adv.*, 5, 65100.
30. Modestov, A. D., Gun, J., Savotina, I. and Lev, O. 2004, *J. Electroanal. Chem.*, 565, 7.
31. Stejskal, J. 2015, *Prog. Polym. Sci.*, 41, 1.
32. Yu, H., Wu, J., Fan, L., Hao, S., Lin, J. and Huang, M. 2015, *J. Power Sources*, 248, 1123.
33. Yu, H.-J., Wu, J.-H., Fan, L.-Q., Lin, Y.-Z., Chen, S.-H., Chen, Y., Wang, J.-L., Huang, M.-L., Lan, Z. and Huang, Y.-F. 2012, *Sci. China Ser. B*, 55, 1319.
34. Su, L., Gong, L., Lu, H. and Xu, Q. 2014, *J. Power Sources*, 248, 212.
35. Yu, H., Fan, L., Wu, J., Lin, Y. and Lan, Z. 2012, *RSC Adv.*, 2, 6736.
36. Wang, Q., Nie, Y. F., Chen, X. Y., Xiao, Z. H. and Zhang, Z. J. 2016, *J. Power Sources*, 323, 8.
37. Zhang, Z. J., Huang, X. and Chen, X. Y. 2015, *RSC Adv.*, 5, 87571.
38. Zhu, Y. Q., Zhang, L., Chen, X. Y., Xiao, Z. H. and Zhang, Z. J. 2015, *J. Power Sources*, 299, 629.
39. Zhang, Z. J., Wang, Q., Zhu, Y. Q. and Chen, X. Y. 2016, *Carbon*, 100, 564.
40. Bornstein, A., Hershkovitz, S., Oz, A., Luski, S., Tsur, Y. and Aurbach, D. 2015, *J. Phys. Chem. C*, 119, 12165.
41. Chun, S.-E., Evanko, B., Wang, X., Vonlanthen, D., Ji, X., Stucky, G. D. and Boettcher, S. W. 2015, *Nat. Commun.*, 6, 7818.
42. Menzel, J., Fic, K., Meller, M. and Frackowiak, E. 2014, *J. Appl. Electrochem.*, 44, 439.
43. Singh, A. and Chandra, A. 2016, *Sci. Rep.*, 6, 25793.
44. Abbas, Q. and Beguin, F., 2015, *Prog. Nat. Sci.*, 25, 622.
45. Chen, K., Liu, F., Xue, D. and Komarneni, S. 2015, *Nanoscale*, 7, 452.
46. Narayanan, R. and Bandaru, P. R. 2015, *J. Electrochem. Soc.*, 162, A86.
47. Lee, J., Choudhury, S., Weingarth, D., Kim, D. and Presser, V. 2016, *ACS Appl. Mater. Interfaces*, 8, 23676.
48. Zhao, C., Zheng, W., Wang, X., Zhang, H., Cui, X. and Wang, H. 2013, *Sci. Rep.*, 3, 2986.
49. Su, L.-H., Zhang, X.-G., Mi, C.-H., Gao, B. and Liu, Y. 2009, *Phys. Chem. Chem. Phys.*, 11, 2195.
50. Shanmugavani, A., Kaviselvi, S., Sankar, K. V. and Selvan, R. K. 2014, *Mat. Res. Bull.*, 62, 161.
51. Abbas, Q., Ratajczak, P. and Beiguin, F. 2014, *Faraday Discuss.*, 172, 199.
52. Diaz, P., Gonzalez, Z., Santamaria, R., Granda, M., Menendez, R. and Blanco, C. 2015, *Electrochim. Acta*, 168, 277.

53. Liu, T., Zhu, Y., Liu, E., Luo, Z., Hu, T., Li, Zi. and Ding, R. 2015, *Trans. Nonferrous Met. Soc. China*, 25, 2661.
54. Pandey, K., Yadav, P. and Mukhopadhyay, I. 2015, *Phys. Chem. Chem. Phys.*, 17, 878.
55. Frackowiak, E., Fic, K., Meller, M. and Lota, G. 2012, *Chem. Sus. Chem.*, 5, 1181.
56. Zhao, Y., Wang, L. and Byon, H. R. 2013, *Nat. Commun.*, 4, 1896.
57. Chen, L., Bai, H., Huang, Z. and Li, L. 2014, *Energy Environ. Sci.*, 7, 1750.
58. Menzel, J., Fic, K. and Frackowiak, E. 2015, *Prog. Nat. Sci.*, 25, 642.
59. Fic, K., Meller, M., Menzel, J. and Frackowiak, E. 2016, *Electrochim. Acta*, 206, 496.
60. Yamazaki, S., Ito, T., Yamagata, M. and Ishikawa, M. 2012, *Electrochim. Acta*, 86, 294.
61. Xie, H. J., Gellnas, B. and Rochefort, D. 2016, *Electrochem. Commun.*, 66, 42.
62. Senthilkumar, S. T., Selvan, R. K., Ponpandian, N. and Melo, J. S. 2012, *RSC Adv.*, 2, 8937.
63. Yu, H., Wu, J., Fan, L., Xu, K., Lin, Y., Lin, J. 2011, *Electrochim. Acta*, 56, 6881.
64. Sun, K., Ran, F., Zhao, G., Zhu, Y., Zheng, Y., Ma, M., Zheng, X., Ma, G. and Lei, Z. 2016, *RSC Adv.*, 6, 55225.
65. Feng, E., Ma, G., Sun, K., Yang, Q. and Lei, Z. 2016, *RSC Adv.*, 6, 75896.
66. Kim, D., Lee, G., Kim, D., Yun, J., Lee, S-S. and Ha, J. S. 2016, *Nanoscale*, 8, 15611.
67. Ran, J., Wu, L., He, Y., Yang, Z., Wang, Y., Jiang, C., Ge, L., Bakangura, E. and Xu, T. 2017, *J. Membrane Sci.*, 15, 267.
68. Ran, J., Wu, L., He, Y., Yang, Z., Wang, Y., Jiang, C., Ge, L., Bakangura, E. and Xu, T. 2017, *J. Membrane Sci.*, 15, 267.
69. Kim, H-J. and Han, Y-K. 2016, *Curr. Appl. Phys.*, 16, 1437.
70. Tomai, T., Mitoni, S., Kamatsu, D., Kawaguchi, Y. and Honma, I. 2014, *Sci. Rep.*, 4, 3591.
71. Shul, G. and Belanger, D. 2016, *Phys. Chem. Chem. Phys.*, 18, 19137.
72. Weinstein, L. and Dash, R. 2013, *Mater. Today*, 16, 356.